doi:10.1016/j.jmb.2005.11.085 J. Mol. Biol. (2006) 356, 746–758

JMB

Available online at www.sciencedirect.com

SCIENCE DIRECT®

ELSEVIER

The Co-chaperone p23 Arrests the Hsp90 ATPase Cycle to Trap Client Proteins

Stephen H. McLaughlin[1]*, Frank Sobott[1], Zhong-ping Yao[1], Wei Zhang[2] Peter R. Nielsen[2], J. Günter Grossmann[3], Ernest D. Laue[2] Carol V. Robinson[1] and Sophie E. Jackson[1]*

[1]*Cambridge University Chemical Laboratory, Lensfield Road, Cambridge CB2 1EW UK*

[2]*Department of Biochemistry University of Cambridge Tennis Court Road, Cambridge CB2 1GA, UK*

[3]*Synchrotron Radiation Department, CCLRC Daresbury Laboratory, Daresbury Warrington WA4 4AD, UK*

**Corresponding authors*

The action of the molecular chaperone Hsp90 is essential for the activation and assembly of an increasing number of client proteins. This function of Hsp90 has been proposed to be governed by conformational changes driven by ATP binding and hydrolysis. Association of co-chaperones and client proteins regulate the ATPase activity of Hsp90. Here, we have examined the inhibition of the ATPase activity of human Hsp90β by one such co-chaperone, human p23. We demonstrate that human p23 interacts with Hsp90 in both the absence and presence of nucleotide with a higher affinity in the presence of the ATP analogue AMP-PNP. This is consistent with an analysis of the effect of p23 on the steady-state kinetics that revealed a mixed mechanism of inhibition. Mass spectrometry of the intact Hsp90.p23 complex determined the stoichiometry of binding to be one p23 to each subunit of the Hsp90 dimer. p23 was also shown to interact with a monomeric, truncated fragment of Hsp90, lacking the C-terminal homodimerisation domain, indicating dimerisation of Hsp90 is not a prerequisite for association with p23. Complex formation between Hsp90 and p23 increased the apparent affinity of Hsp90 for AMP-PNP and completely inhibited the ATPase activity. We propose a model where the role of p23 is to lock individual subunits of Hsp90 in an ATP-dependent conformational state that has a high affinity for client proteins.

Keywords: molecular chaperone; Hsp90; heat shock; protein folding; p23

Introduction

A wide range of proteins are dependent on the abundant cytosolic molecular chaperone Hsp90 for their maturation and activation.[1–5] At present, over 100 such Hsp90 substrate or client proteins have been reported, many of which are involved in fundamental cellular processes such as transcriptional regulation, cell cycle, and signal transduction†. This may be a conservative estimate, as recent genome-wide analyses in yeast reveal there are upward of 600 potential client proteins or co-chaperones representing between 3% and 10% of the yeast proteome.[6,7]

The function of Hsp90 is dependent on its ability to bind and hydrolyse ATP.[8,9] Though Hsp90 displays only a weak ATPase activity, the rate at which it cycles is critical for its function *in vivo*.[10] The molecular mechanism by which ATP turnover regulates Hsp90 is unclear. Hsp90 is a multi-domain protein consisting of three domains: an N-terminal ATP-binding domain (N); a middle region (M); and a C-terminal homodimerisation domain (C) containing a tetratricopeptide repeat (TPR) protein-binding motif.[2] ATP binding changes the global properties of the protein, such as a reduction in hydrophobicity implying conformational changes or domain reorganization.[11] It is thought that the ATP turnover rate governs the time that a client protein remains bound by Hsp90.[10,12,13] In support of such a mechanism, human Hsp90 has been shown to have a higher affinity for a client protein in

Abbreviations used: SPR, surface plasmon resonance; nanoESI-MS, nano-electronspray ionization mass spectrometry; AUC, analytical ultracentrifugation; SAXS, small-angle X-ray scattering; ITC, isothermal titration calorimetry.

E-mail addresses of the corresponding authors: smclaugh@ntlworld.com; sej13@cam.ac.uk

† For an update, see http://www.picard.ch/downloads/downloads.htm

the ATP-bound state than in the ADP-bound state.[14] The ATPase activity of Hsp90 is regulated by the transient association with a variety of co-chaperones[13,15–17] as well as by the binding of client proteins.[13,14]

The small acidic co-chaperone p23 has been shown to inhibit the ATPase activity of human Hsp90.[13] It was discovered as part of Hsp90 complexes containing the steroid hormone receptor client proteins and high molecular mass immunophilins, such as Cyp40 and FKBP52.[18–20] These are termed mature complexes, as the steroid hormone receptor client proteins are in a ligand-binding competent conformation.[3,21,22] The role of p23 in these complexes remains unclear and several different functions have been suggested. p23 appears to stabilise the interaction between Hsp90 and a client protein *in vitro*,[23,24] correlating with its ability to increase the activation of heterologously expressed estrogen receptor *in vivo*.[25] In contrast, another study has proposed that p23 is a client protein release factor, linking ATP hydrolysis with client protein dissociation from Hsp90.[12] Beyond acting as a control factor for Hsp90, p23 has been shown to be a molecular chaperone maintaining unfolded proteins in a folding-competent state.[26,27] This implies that p23 may have a direct role in client protein activation. Opposing a role in assisting the assembly process, p23 may alter the transcriptional activity of nuclear receptors by affecting the dissociation rate of the receptor–DNA response element complex.[28]

The molecular mechanism by which p23 acts as a co-chaperone for Hsp90 is unknown. The yeast homologue, Sba1, is non-essential for yeast viability.[29,30] It was thought that p23 binds exclusively to the ATP form of Hsp90,[11,19,31–33] though a weak interaction has been reported recently between Sba1 and a nucleotide-free state of yeast Hsp90.[34] There is inconsistency regarding the level of inhibition that p23 can elicit. While p23 has been found to partially inhibit the basal ATPase activity of Hsp90,[13,33,34] more extensive inhibition was observed in the presence of a client protein and the co-chaperone FKBP52.[13] In conflict with these studies, it has been reported that Sba1 has no effect on either the activity or steady-state kinetics of yeast Hsp90 ATPase.[12]

The position and nature of the interaction between p23 and Hsp90 are unknown. A yeast two-hybrid screen indicated that only full-length Hsp90 was capable of interacting with p23.[9] Evolutionary tracing coupled with protein-docking programs have modelled the putative interface between Hsp90 and p23 to be within the N-terminal domain, with p23 binding over the nucleotide-binding site.[35] These coincide with the one face of p23 that mutant studies have implicated in the Hsp90 interaction.[36,37] Deletion studies have shown that both the N-terminal and the middle domains of Hsp90 are required for interaction with p23, and the truncated monomers need to be in close proximity, either by expression with a dimeric fusion protein[38] or chemical cross-linking.[10] There is controversy regarding the stoichiometry of the interaction between yeast p23 and yeast Hsp90, with either a 1:2[34] or 1:1[33] molar ratio (p23:Hsp90) implying either a symmetric or asymmetric p23.Hsp90 complex.

Here, we have investigated the interaction of human p23 with both full-length and a monomeric fragment of human Hsp90β in the absence and in the presence of nucleotides. The stoichiometry of the interaction was determined by mass spectrometry of intact p23.Hsp90 complexes. The effect of p23 on the steady-state kinetics of the ATPase activity of Hsp90 was analysed to determine the mechanism of inhibition. The results have led us to propose a new model for the role of p23 in the human Hsp90 ATPase cycle.

Results

Human p23 binds to both nucleotide-bound and nucleotide-free Hsp90

The interaction of p23 with Hsp90 has been demonstrated to be nucleotide-dependent.[11,31–34] To quantify the effect of nucleotide on the kinetics and binding affinity of the interaction between human p23 and human Hsp90, p23 was coupled to the surface of a sensor chip and complex formation was monitored by surface plasmon resonance (SPR) in the absence and in the presence of the non-hydrolysable ATP analogue AMP-PNP and ADP.

Contrary to previous reports, binding of p23 to Hsp90 was detected in the presence and in the absence of both ADP and AMP-PNP (Figure 1(a)). At 25 °C, the nucleotide-free and ADP-bound state of Hsp90 have a similar affinity for p23, with dissociation constants of 17 μM and 10 μM, respectively. Addition of AMP-PNP to Hsp90 increases the affinity for p23 by an order of magnitude, with a dissociation constant for the complex of 1.5 μM. Increasing the temperature to 37 °C reduced the stability of the complex for both the nucleotide-free and AMP-PNP bound states (Table 1).

Using SPR, the effect of nucleotide on the binding kinetics could be examined and individual rate constants measured (Table 1). The absence or the presence of ADP appeared to have little effect on the kinetics of dissociation with off-rate constants of $7.0\times10^{-3}\,s^{-1}$ and $9.2\times10^{-3}\,s^{-1}$, respectively. The presence of AMP-PNP decreased the dissociation rate approximately threefold, to $3.0\times10^{-3}\,s^{-1}$ at 25 °C. However, this effect was reversed at 37 °C, with a higher dissociation rate constant of $1.7\times10^{-3}\,s^{-1}$ in the presence of AMP-PNP compared to $1.0\times10^{-3}\,s^{-1}$ in its absence (data not shown; and see Table 1). A more dramatic effect of AMP-PNP on the association rate was observed. The association rate constant in the presence of AMP-PNP increases between fivefold and 11-fold, at 25 °C and 37 °C, respectively, compared to nucleotide-free Hsp90.

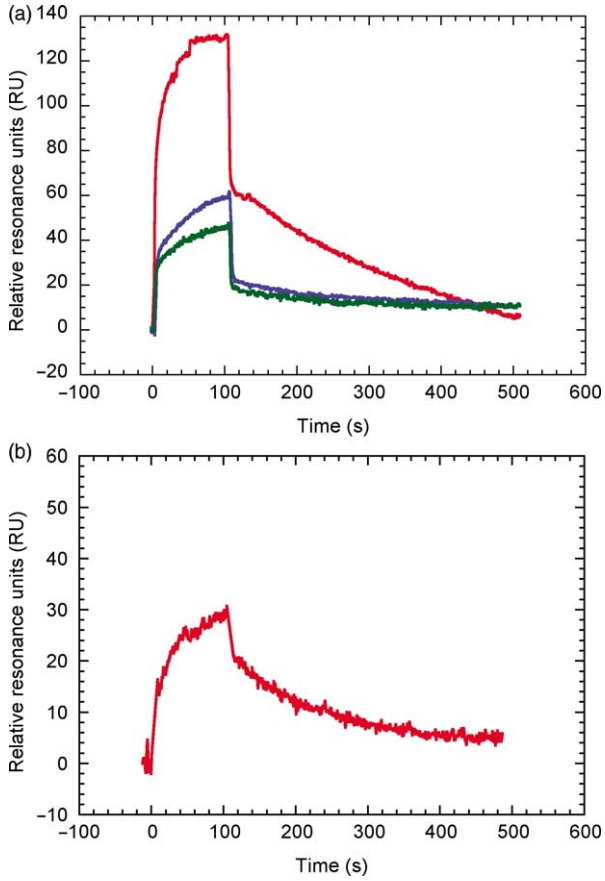

Figure 1. Interaction between Hsp90 and p23 analysed by SPR. (a) Association and dissociation of 25 μM Hsp90 from the surface of a p23-coupled sensor chip in the absence (blue) and in the presence (green) of 2 mM ADP and AMP-PNP (red) at 25 °C. (b) Association and dissociation of 100 μM Hsp90ΔC from the surface of a p23-coupled sensor chip in the presence of 2 mM AMP-PNP (red) at 25 °C. Dissociation rate constants were obtained by fitting the dissociation phase to a single-exponential function. Association rate constants were obtained by fitting data to equation (1).

p23 interacts with monomeric Hsp90ΔC

The subunits of the Hsp90 dimer are associated *via* the C-terminal domains.[39] It has been postulated that either N-terminal proximity or an N-terminally dimerised form of Hsp90 is essential for the interaction with p23.[10,33,38] Recently, however, we have shown that there is no evidence for an ATP-induced N-terminally dimerised conformational change in human Hsp90β.[14] Therefore, to investigate the role of the oligomeric status of Hsp90 on complex formation, we examined the association of p23 with a monomeric C-terminally truncated Hsp90 fragment (Hsp90ΔC) using SPR. Figure 1(b) shows that in the presence of AMP-PNP, p23 interacts with Hsp90ΔC. The reduction in the change in resonance reflects a weaker interaction with an approximately 20-fold increase in the dissociation constant (33 μM) at 25 °C. Similarly, there were significant changes in the binding kinetics with association and dissociation rate constants more akin to the nucleotide-free and ADP-bound states (Table 1).

The oligomeric status of p23

In order to obtain accurate stoichiometric data for the complex between Hsp90 and p23, it was necessary to determine the oligomeric status of p23. Size-exclusion chromatography experiments under reducing conditions (Figure 2) revealed that full-length p23 eluted with an apparent molecular mass of 37 kDa, approximately twice the expected size of the calculated mass of 18.9 kDa. In comparison, p23ΔC eluted as a monomer with an apparent mass of 19 kDa, close to the expected mass of 15.5 kDa. Incubation of full-length p23 in the absence of reducing agent resulted in the appearance of higher oligomeric species, accompanied by the decrease in the apparent dimeric peak. This indicated that p23 undergoes aberrant disulfide bond formation under non-reducing conditions. The crystal structure of the globular domain of p23 (p23ΔC) revealed that under appropriate conditions, p23 could dimerise *via* an aberrant disulfide bond.[40] To ascertain if the apparent dimeric p23 was due to a disulfide bond that was resistant to reduction by DTT, the molar ratio of cysteine was measured using modification with 5,5′-dithiobis(2-nitrobenzoic acid) under native and denaturing conditions. In both the absence and the presence of 6 M GdnHCl, where p23 is completely denatured as judged by fluorescence emission (data not shown), all five cysteine residues per p23 monomer were modified, indicating that there were no disulfide bonds linking the apparent dimer.

The oligomeric state of full-length p23 was investigated further by nano-electronspray ionisation mass spectrometry (nanoESI-MS), analytical ultracentrifugation and small-angle X-ray scattering (SAXS). The inset in Figure 3(b) shows the nanoESI mass spectrum for full-length p23 using

Table 1. Kinetic and thermodynamic parameters of the p23 and Hsp90 interaction

Protein	T (°C)	Nucleotide	K_d (μM)	k_{on} ($M^{-1}\,s^{-1}$)	k_{off} (s^{-1})
Human Hsp90	25		17	420±30	$7.0(\pm0.2)\times10^{-3}$
	25	ADP	10	900±100	$9.2(\pm1.2)\times10^{-3}$
	25	AMP-PNP	1.5	$2.0(\pm0.5)\times10^{3}$	$3.0(\pm0.1)\times10^{-3}$
	37		31	330±110	$1.0(\pm0.3)\times10^{-2}$
	37	AMP-PNP	4.5	$3.8(\pm0.4)\times10^{3}$	$1.7(\pm0.1)\times10^{-2}$
Human Hsp90ΔC	25	AMP-PNP	33	250±25	$8.1(\pm0.2)\times10^{-3}$

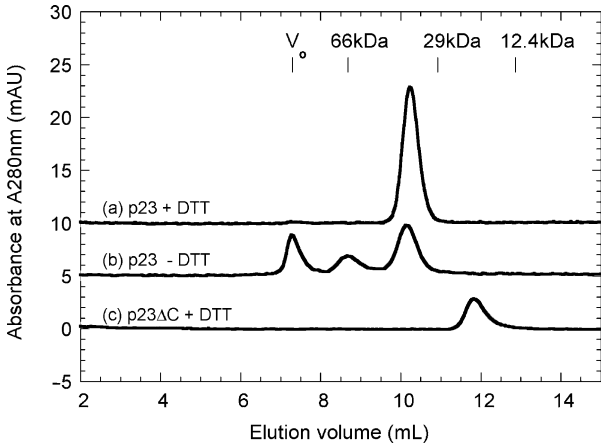

Figure 2. Size-exclusion chromatography of p23 under reducing and non-reducing conditions. The oligomeric status of 7 μM full-length p23 and p23ΔC were examined by gel-filtration chromatography on a Sephadex S75 HR10/30 column. Parallel samples of full-length p23 were incubated for 90 min at 25 °C (a) in the presence or (b) in the absence of 10 mM DTT before elution and compared to (c) p23ΔC incubated with 10 mM DTT. Molecular mass was calculated by comparing the relative elution (equation (2)) with those of standard proteins.

conditions optimised for the transmission of non-covalent complexes. There was only one set of peaks between 2000 m/z and 3000 m/z, with no other significant peak visible in the spectrum. These peaks correspond to charge states of a protein with a mass of 18,977 Da, which compares well with the theoretical mass of 18,978.6 Da, indicating that p23 is monomeric under these conditions. Under non-reducing conditions, using higher concentrations of p23 (up to 50 μM), additional peaks could be observed that correspond to a dimer of p23 (data not shown). However, collision-induced dissociation experiments showed fragmentation of the dimer into peptide fragments (data not shown). If the species were a non-covalently bound dimer, we would anticipate dissociation into subunits prior to fragmentation of the peptide bonds. Sedimentation equilibrium analytical ultracentrifugation showed that p23 and p23ΔC were monomeric and there was no shift in M_r for concentrations up to 150 μM and 130 μM, respectively (data not shown). SAXS confirmed that p23 is a monomer in solution up to concentrations of 130 μM (data not shown).

Together, these data indicate that measurement of the oligomeric status of full-length p23 by size-exclusion chromatography is inaccurate. The appar-

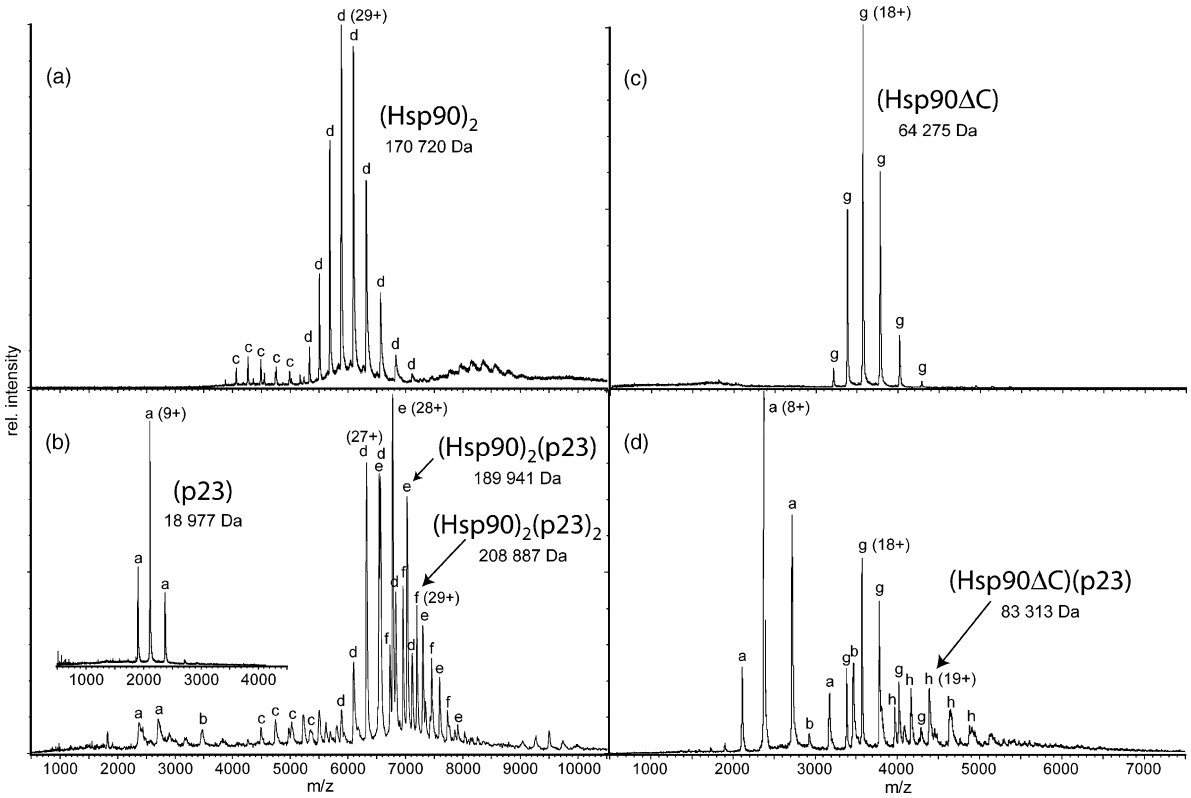

Figure 3. NanoESI mass spectra for solutions of (a) Hsp90, (b) Hsp90 and p23, (c) Hsp90ΔC, and (d) Hsp90ΔC and p23. The inset in (b) shows the spectrum for p23 alone. The ion series a, b, c, d, e, f, g and h corresponds to species (p23), $(p23)_2$, (Hsp90), $(Hsp90)_2$, $(Hsp90)_2(p23)$, $(Hsp90)_2(p23)_2$, (Hsp90ΔC) and (Hsp90ΔC)(p23), respectively. The major charge states for each species are labelled in parentheses. The spectra were typically acquired at a capillary voltage of 2000 V and a cone voltage of 200 V, with a sample concentration of 20 μM. Pressures inside the mass spectrometer were optimized for transmission of non-covalent complexes.

ent dimeric molecular mass calculated from size-exclusion chromatography is most likely due to the unstructured C-terminal acidic tail of p23 increasing the apparent diameter of p23.[41] This would give rise to an aberrant elution profile during size-exclusion chromatography, as observed. While p23 is monomeric under reducing conditions, it is prone to formation of a non-native disulfide-linked dimer under oxidizing conditions. Consequently, care was taken in all experiments to ensure that the p23 was maintained under reducing conditions.

Two molecules of p23 bind to the human Hsp90 dimer

To establish the constituents of the complex between human p23 and human Hsp90, we took advantage of the ability of nanoESI-MS to maintain complexes intact and observe the presence of non-native disulfide bond formation in p23. Experimental conditions were optimised to maintain the Hsp90 in the dimeric form (Figure 3(a)). Spectra recorded after the incubation of p23 and Hsp90 in the absence of added nucleotide (Figure 3(b)) resulted in the appearance of an additional group of peaks in the region of 6000–7000 m/z that are not present in the spectra of the individual proteins (Figure 3(a) and (b), inset). These peaks are assigned to a complex formed between Hsp90 and p23 with ratios of 2:1 and 2:2 (see Table 2). Similar molar ratios were obtained with truncated p23ΔC (data not shown, Table 2), indicating removal of the acidic tail of p23 does not eliminate the interaction. To examine the possibility that the higher stoichiometry was due to a disulfide-linked dimer of p23 binding to the dimer of Hsp90, experimental conditions were chosen that cause the Hsp90 dimer to dissociate in the gas phase. This revealed a 1:1 complex with p23 (data not shown). The spectrum of truncated Hsp90ΔC showed a shift to lower m/z values (Figure 3(c)) consistent with it existing as a monomer in solution.[14] Analysis of the spectrum of an equimolar mixture of p23 and Hsp90ΔC was consistent with the formation of a 1:1 complex (Figure 3(d)). A dimeric species of Hsp90ΔC in the presence of p23 was not observed. The extent of binding here seems considerably reduced when compared to the full-length protein, which reflects the weaker affinity of the interaction between p23 and Hsp90ΔC shown by SPR (Figure 1(b)). The effect of bound nucleotide on complex formation was examined using a tenfold molar excess of nucleotide over protein. There was no change in the stoichiometry observed upon addition of nucleotide (data not shown). It was not possible to use higher concentrations of nucleotide that would saturate Hsp90, as high levels of non-volatile salt both suppressed the ion signal and decreased the resolution, as the binding of a distribution of cations broadens the peaks in the mass spectra.

Table 2. Stoichiometry of p23.Hsp90 complexes

Protein	p23	p23ΔC
Hsp90	(90)(23)	(90)(23ΔC)
	$(90)_2(23)$	$(90)_2(23\Delta C)$
	$(90)_2(23)_2$	$(90)_2(23\Delta C)_2$
Hsp90ΔC	(90ΔC)(23)	(90ΔC)(23ΔC)

Complete inhibition of Hsp90 ATPase activity by p23

We have shown that human p23 inhibits both the basal and the client protein-stimulated ATPase activity of Hsp90.[13] There was a distinct difference in the effect of p23 on both rates: only a modest suppression in the basal ATPase activity was apparent compared with a reduction of the client-stimulated rate to basal levels. This compares well with recent studies where Sba1 inhibits yeast Hsp90 basal ATPase activity to only approximately 50% of its initial value in the absence of Sba1.[33,34] However, in light of the binding affinities of human p23 to Hsp90 measured here (Table 1), the concentrations of human p23 used in our previous study would not have been enough to reach saturation. Hence, it has been necessary to re-investigate the effect of p23 on the basal ATPase activity of human Hsp90.

Figure 4(a) shows the p23 concentration-dependence of human Hsp90 ATPase activity at 37 °C in the absence of any client protein. At relatively low concentrations of p23, where the client protein-stimulated rate was inhibited,[13] we again see only modest reductions in activity, consistent with our previous study. Increasing the concentration of p23 to between eightfold and tenfold molar excess over Hsp90, however, completely inhibits the ATPase activity, with an IC_{50} of approximately 5 μM. This value is in good agreement with the K_d of 4.5 μM measured by SPR in the presence of AMP-PNP at 37 °C (Table 1).

The analysis of the interaction of p23 and Hsp90ΔC in the presence of AMP-PNP showed that both the kinetics and binding affinity were of the same order as the binding of p23 to full-length Hsp90 in either the ADP or nucleotide-free states. This may imply that the interaction between p23 and the monomeric Hsp90 fragment is uncoupled from the nucleotide status of the N-terminal domain. As Hsp90ΔC hydrolyses ATP,[14] albeit more weakly than full-length Hsp90, we could investigate if p23 inhibits the active conformation of Hsp90. In comparison to full-length Hsp90, Figure 4(b) shows that higher concentrations of p23 were needed to inhibit Hsp90ΔC to a similar level, with a corresponding increase in the IC_{50} to 17 μM at 37 °C.

Mechanism of p23 inhibition of the steady-state kinetics of Hsp90 ATPase

Current models of the interaction of Hsp90 with p23 predict several possible mechanisms of inhibition. If p23 interacts only with the ATP-bound

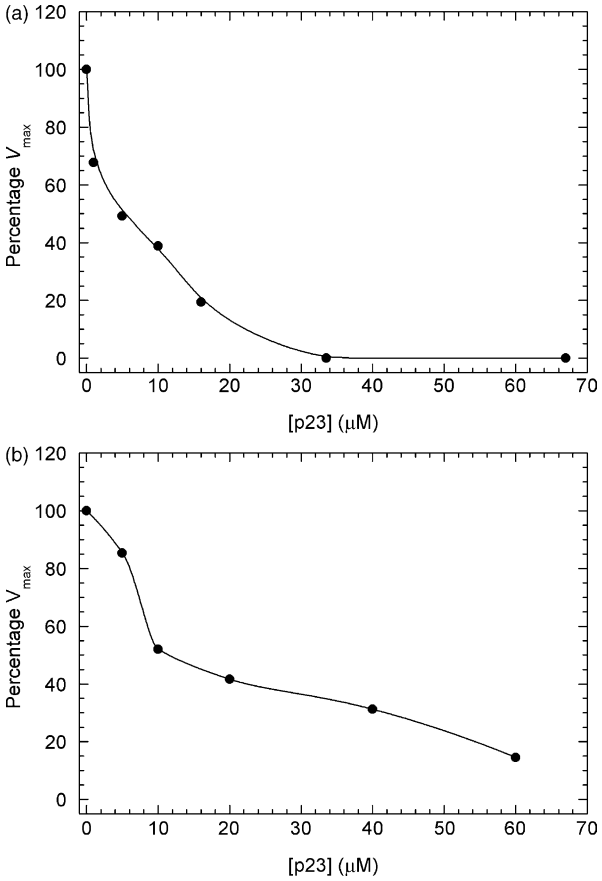

Figure 4. Complete inhibition of the steady-state ATPase activity of Hsp90 by p23. The ATPase activity of (a) 5 μM human Hsp90β and (b) 5 μM human Hsp90ΔC were measured at 37 °C in the presence of increasing concentrations of full-length human p23.

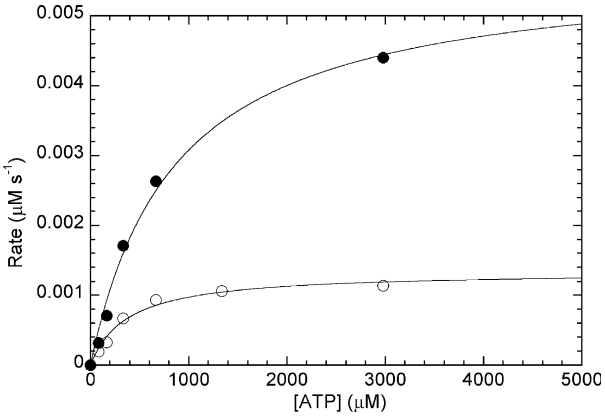

Figure 5. Effect of p23 on the steady-state kinetics of human Hsp90β ATPase activity. The Michaelis–Menten kinetics of the ATPase activity of 10 μM human Hsp90β were measured in the absence (filled circles) and in the presence (open circles) of 10 μM human p23. The best fit of the data to the standard Michaelis–Menten equation is shown by the continuous lines, which yield values of $K_m = 860(\pm 100)$ μM and $k_{cat} = 5.7(\pm 0.1) \times 10^{-4}\ s^{-1}$ in the absence of p23, and $K_m = 370(\pm 60)$ μM and $k_{cat} = 1.3(\pm 0.2) \times 10^{-4} s^{-1}$ in the presence of p23.

state of Hsp90 and inhibits activity completely, theory would predict that both the steady-state Michaelis–Menten parameters k_{cat} and K_m are decreased by a factor of $(1+[I]/K_I)$, where [I] is the concentration of p23 and K_I is the dissociation constant for the p23.Hsp90 complex in the presence of ATP. Hence, for such an uncompetitive mechanism, the ratio of k_{cat}/K_m would remain constant. Alternatively, if p23 binds to both the nucleotide-free and ATP-bound state of Hsp90, as shown in Figure 1, then k_{cat} will decrease by a factor of $(1+[I]/K_I)$ and K_m will decrease by a factor of $[(1+[I]/K_I)/(1+[I]/K'_I)]$, where K'_I is the dissociation constant of the complex in the absence of bound nucleotide.

Figure 5 shows the rate of inorganic phosphate release from human Hsp90 as a function of ATP concentration in the absence and presence of human p23. The concentration of p23 was approximately twofold above the K_I and threefold below K'_I. Michaelis–Menten analysis revealed that in the presence of p23, K_m is reduced by approximately twofold from $860(\pm 100)$ μM to $370(\pm 60)$ μM, and k_{cat} is reduced fourfold from $5.7(\pm 0.1) \times 10^{-4}\ s^{-1}$ to $1.3(\pm 0.2) \times 10^{-4}\ s^{-1}$ at 37 °C. As the ratio of k_{cat}/K_m is not constant, these data point towards a mixed-inhibition mechanism, consistent with the SPR data on the interaction of p23 with both the unbound and ATP-bound states of Hsp90.

The effect of p23.Hsp90 complex formation on the apparent nucleotide affinity of Hsp90

The reduction of K_m in the presence of p23 should be reflected in a change in the apparent dissociation constant for ATP. Therefore, we examined the binding of the non-hydrolysable ATP analogue AMP-PNP to Hsp90 by isothermal titration calorimetry at 25 °C (Figure 6) in the presence of p23. AMP-PNP was titrated into a cell containing the Hsp90.p23 complex. When data were fit with three floating variables: stoichiometry, dissociation binding constant, K_{obs}, and the change in enthalpy of interaction, AMP-PNP was determined to bind with a dissociation constant, K_{obs} of $39(\pm 12)$ μM at a stoichiometry of 0.8 ± 0.2 to each Hsp90 subunit. This is compared to a value of 148 μM at 25 °C measured in the absence of p23.[14]

The apparent reduction in the dissociation constant for AMP-PNP binding does not necessarily imply that p23 affects the nucleotide affinity of Hsp90 directly. In the presence and in the absence of p23, the binding of nucleotide to Hsp90 can be analysed using two alternative thermodynamic schemes (Figure 6(b)): (I) in which the Hsp90.p23 complex binds ligand with a dissociation constant $K'_{AMP-PNP}$; or (II) the Hsp90.p23 complex cannot bind nucleotide. A recent computer model of the docking between the proteins proposed that

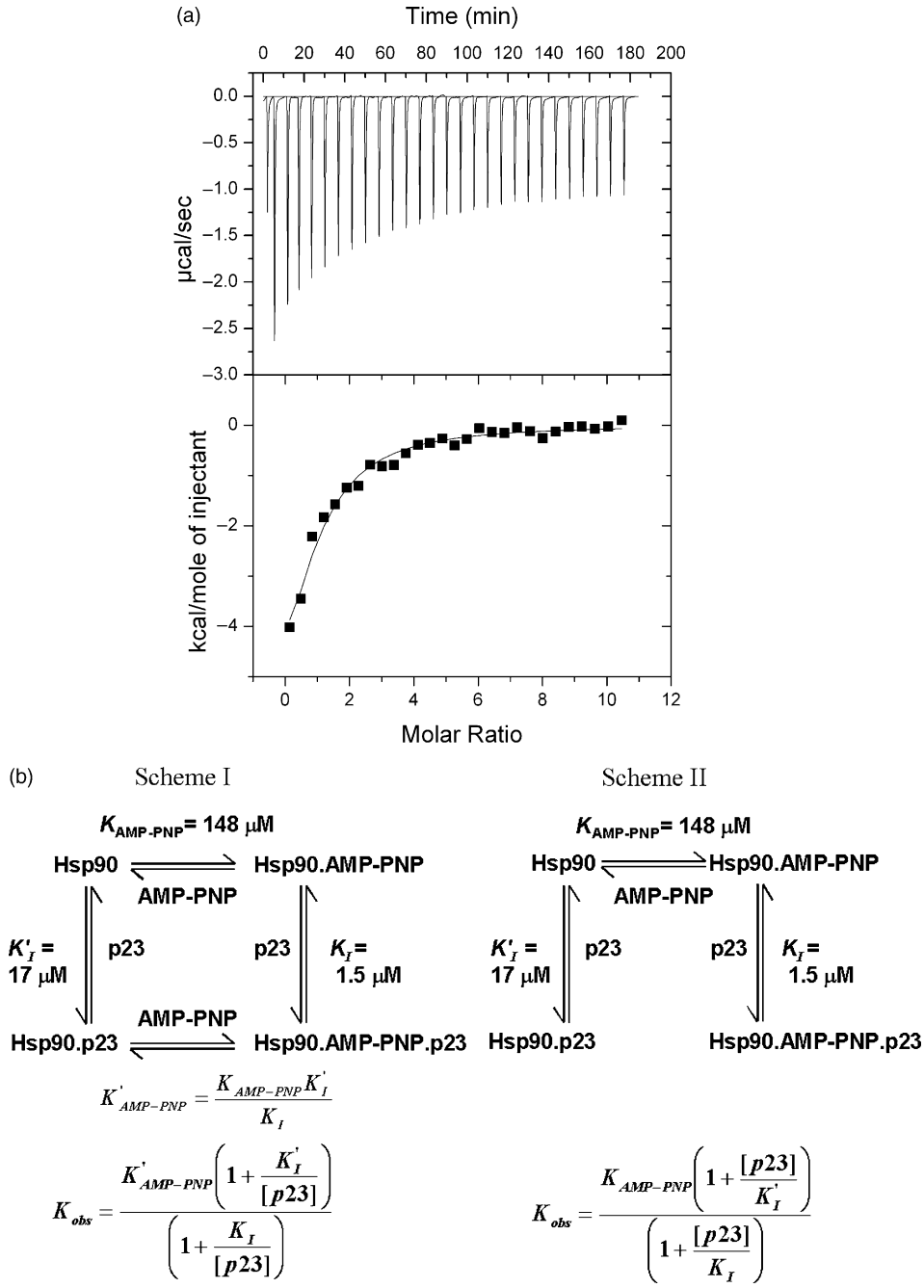

Figure 6. Isothermal titration calorimetry of AMP-PNP binding to Hsp90.p23 complex. (a) AMP-PNP was injected into a cell containing full-length human Hsp90β and p23 at 25 °C. Nucleotide bound with a stoichiometry of 0.8 ± 0.2 to each Hsp90 subunit with a K_d of 39(±12) µM. (b) Alternative thermodynamic schemes for the binding of p23 and nucleotide to Hsp90.

p23 binds to the N-terminal domain of Hsp90 in an orientation over the nucleotide-binding pocket.[35] It was suggested that the closure of the DNA gyrase-like "ATP-lid" provides an additional interaction surface. Such a model favours scheme II.

In both schemes, the observed dissociation constant for AMP-PNP, K_{obs}, measured by isothermal titration calorimetry (ITC), is dependent on the free concentration of p23, K_I and K'_I the dissociation constants for the Hsp90.p23 complex in the presence and in the absence of AMP-PNP, respectively. In scheme I, the dissociation constant for AMP-PNP binding to the Hsp90.p23 complex, $K'_{AMP-PNP}$, can be calculated from K_{obs}, using the known values of [p23], K_I and K'_I. The value of $K'_{AMP-PNP}$ of 32 µM obtained is significantly higher than a value of 13 µM expected from the ratio of the dissociation constants in the thermodynamic cycle. Therefore, if this scheme is correct, p23 increases the affinity of Hsp90 for AMP-PNP. In scheme II, where AMP-PNP cannot bind directly to the Hsp90.p23 complex, the apparent reduction in the affinity of Hsp90 for AMP-PNP in the presence of p23 is due to the

relatively higher affinity of the Hsp90.AMP-PNP complex for p23. The observed binding constant is approximately twofold above the theoretical binding constant of 16 μM, calculated using the equation. However, the difference in these values may reflect the relatively large error in K_{obs}. It is important to note that the current experiment cannot distinguish which scheme is correct and it remains possible that both pathways for nucleotide binding are available.

Discussion

Here, we have sought to understand the role of p23 as a component of the Hsp90 chaperone machine by characterizing its interaction with Hsp90 and its mechanism of inhibition on the ATPase activity of Hsp90. p23 is found in association with the mature Hsp90.steroid hormone receptor complexes that are poised for activation. By understanding how p23 inhibits the ATPase activity of Hsp90, we hoped to gain an insight into the relationship between the ATP-driven Hsp90 chaperone cycle and client protein association.

Contrary to previous studies,[10,11,32,33,38,42] human p23 was found to interact with both the nucleotide-free and ADP-bound forms of human Hsp90, in addition to the ATP-bound state. The relative binding affinities to the unbound and ATP-bound state of human Hsp90 are consistent with a mixed mechanism of inhibition for p23 on the ATPase activity of Hsp90. Previous studies captured the interactions of human p23 with Hsp90 by immunoprecipitation. One possible explanation for their failure to detect interactions in the absence of ATP, may be due to the change in kinetics. The slower rate of association coupled with a higher rate of dissociation in the absence of ATP would lead to lower levels of complex formation and to greater losses during subsequent processing stages. In accordance with this present study, a relatively weak interaction between Sba1 and yeast Hsp90 in the absence of nucleotides has been detected by ITC with a K_d of 120 μM,[34] compared to the K_d of 17 μM for the human proteins.

The nature of the complex between the yeast Hsp90 and Sba1 is controversial. At present, a stoichiometry of either 1:1 or 1:2 (Sba1:yHsp90) molar ratio has been reported.[33,34] In this study, we demonstrated by nanoESI-MS that both subunits of human Hsp90 can bind human p23 simultaneously giving a stoichiometry of 1:1 for the complex in agreement with one study on the yeast proteins.[33] We found that p23 is exclusively monomeric under reducing conditions. In the absence of reducing agents, however, we observed that human p23 has a tendency to form aberrant disulfide bonds, as revealed in the crystal structure of the globular domain of p23.[40] It is possible that a similar problem with yeast p23 may account for the apparent discrepancy between the measurements of stoichiometry.[33,34]

A dimeric form of Hsp90 was not required for the interaction with p23. Contrary to previous studies with chicken Hsp90α,[38] deletion of the C-terminal homodimerisation domain of human Hsp90 does not prevent the interaction with p23 as judged by SPR, nanoESI-MS, and inhibition assays. Neither did we observe that p23 induces dimerisation of Hsp90ΔC (Figure 3(d)). We have previously demonstrated that Hsp90ΔC is monomeric in the presence of ATP.[14] The association cannot be reliant upon transient dimerisation of the N-terminal domains as postulated for yeast Hsp90,[10] as our previous kinetic analysis of human Hsp90 found no evidence for such a conformational change for the full-length protein or the Hsp90ΔC fragment. Similarly, an SAXS study on human Hsp90 did not detect any gross change in the shape of human Hsp90 on AMP-PNP binding that N-terminal dimerisation would predict.[17] However, the interaction of p23 with Hsp90ΔC was found to be approximately 20-fold weaker than with full-length Hsp90. It should be noted that the ATPase activity of this fragment is an order of magnitude lower than that of the full-length Hsp90,[14] suggesting that conformational changes linked to ATP hydrolysis are closely linked to the p23 interaction. Evidence for this has come from a study of the yeast proteins, where Sba1 was found to bind relatively weakly to mutants of full-length Hsp90 with reduced ATPase activity, even though ATP affinity was unaffected.[34]

The action of human p23 in inhibiting Hsp90 ATPase activity must be discussed in the context of the current knowledge of the conformational changes that occur during the ATPase cycle of human Hsp90 (Figure 7). Our recent kinetic dissection of the kinetics of the human Hsp90 ATPase activity, demonstrated that the rapid diffusion-limited binding of ATP to the N-terminal domain is followed by a slower conformational change prior to the rate-limiting step of ATP hydrolysis.[14] ATP-binding in the N domain has been suggested to induce closure or movement of an "ATP-lid"[10] over the nucleotide-binding pocket, similar to the case of DNA gyrase B,[43] exposing an interface for dimerisation of the N domains.[10,44] Subsequently, the N and M domains are predicted to associate and act as a switch in the conformation of a loop in the M domain that brings catalytic residues close to the ATP-binding pocket for efficient hydrolysis.[45] The recent crystal structure of the N–M domain fragment of the *Escherichia coli* Hsp90 homologue, HtpG,[46] provides the first high-resolution structural evidence for the nature of the conformational change in the presence of nucleotide. Though the ATP-lid region was disordered, there was no apparent closure over the nucleotide-binding pocket. Instead, both the N and M domains are involved in the formation of the nucleotide-binding pocket. In the presence of ADP, the M domain "catalytic loop" was distant from the active site, implying either substantial rearrangements of the inter-domain contacts or an alternative role for this region in the ATPase activity.

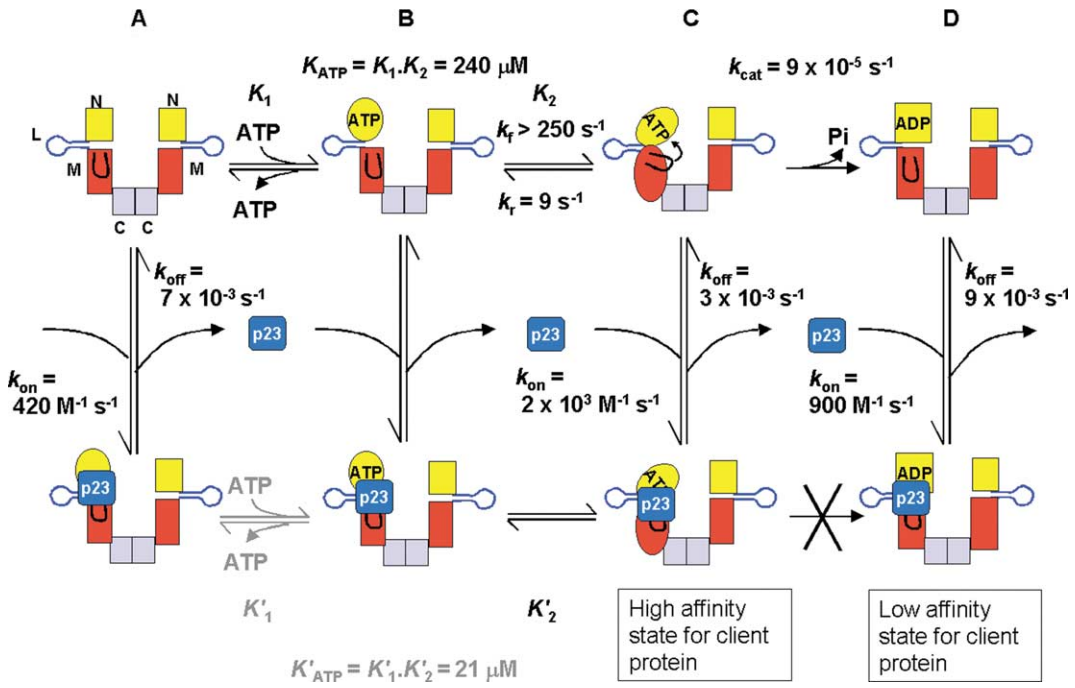

Figure 7. Kinetic model of the inhibition of human Hsp90 ATPase cycle by human p23. Kinetic constants for the reaction in the absence of p23 were measured previously at 25 °C.[14] ATP binding in the N domain of Hsp90 (A to B) induces several conformational changes, possibly involving the "ATP-lid" in the N-terminal domain and contact between the N and M domain (B to C). This state has a high affinity for client proteins. The rate-limiting step is the hydrolysis of ATP (C to D), possibly involving re-arrangement of a catalytic loop in the M domain. Conversion to the ADP-bound state lowers the affinity for a client protein. Rapid dissociation of ADP allows recycling of Hsp90. p23 can bind to all the states of Hsp90 (A to D). The possible interaction with both the M and N domains may increase the affinity of Hsp90 for ATP (A to C). This step is shown in grey as it is not known whether the Hsp90.p23 complex can bind nucleotide. p23 may prevent the hydrolysis reaction (C) by restricting movement of the catalytic loop or rearrangement of the N–M contact. This maintains Hsp90 in a conformation with a high affinity for client proteins until the cycle progresses by either association of other co-chaperones and client proteins that stimulate hydrolysis or by dissociation of p23 from Hsp90.

For human Hsp90, the hydrolysis step is the rate-limiting step in the ATP cycle, switching the conformation of Hsp90 from a high-affinity state for client proteins to a low-affinity state.[14] As the ATPase cycle for human Hsp90 does not involve N-terminal dimerisation, nor is there any evidence that human p23 itself is a dimer or bridges the two subunits of Hsp90 as previously proposed,[14] we will consider, for simplicity, the interaction between one subunit of Hsp90 and p23 (Figure 7).

While both the N and M domains are required for the interaction with p23, it is unclear whether p23 binds to both domains or to a conformation of one domain that is induced by inter-domain association. Some information on the site of interaction can be gleamed by comparison with the association with other co-chaperones. Computer modelling predicts that the interaction site[35] overlaps the interface between the co-chaperone Cdc37 and the N-terminal domain of yeast Hsp90.[47] However, there is debate as to whether p23 competes with Cdc37,[34] or binds at a different site.[48,49] While Cdc37 binds to the N-terminal domain and charged linker region of Hsp90,[17] p23 fails to interact with this fragment.[38] The co-chaperones Aha1 and HOP have been shown to compete with p23 for interaction with Hsp90.[48] While HOP has been proposed to interact with both the C and N domains,[15.] Aha1 binds only to the M domain of Hsp90.[50] These results imply that p23 interacts with both the N and M domains of Hsp90. Important caveats in interrupting competition experiments are that co-chaperone binding may elicit conformational changes that mask the interaction surface for p23 or interactions between co-chaperones may be in direct competition.[51] The interaction of p23 with both the N and M domains of Hsp90 may account for the lower affinity between p23 and Hsp90ΔC. As optimal ATPase activity involves interactions between the N and M domains of Hsp90,[50] the reduced activity of Hsp90ΔC may be reflected in a change in the kinetics of domain association, leading to a weaker interaction with p23.

In the presence of p23, the ATPase cycle of human Hsp90 is completely inhibited. Two possible mechanisms for p23 inhibition are either it prevents the association of the N and M domains or it prevents the movement of the M domain "catalytic loop". SAXS studies reveal that, in absence of co-factors, human Hsp90 appears to exist in an ensemble of conformational states, indicating a flexible and dynamic dimer.[17] It can be envisioned that this

may involve multiple configurations of the N and M domains from open to closed. Association of p23 could prevent conversion of the open form to the closed form, or stabilise the contacts between the N and M domains in the closed form. In the latter case, it might be expected that p23 would actually increase the ATPase activity. The inhibition by p23 suggests it may prevent a further conformational change linked directly to hydrolysis, such as movement of the catalytic loop into the active site in opposition to the action of the co-chaperone Aha1.[50] It is of note that Sba1 has been demonstrated to interact with yeast Hsp90 in the presence of a transition-state analogue of ATP hydrolysis.[33] While the molecular detail of the interaction of p23 and Hsp90 awaits further investigation, we have shown here that the function of p23 is to lock human Hsp90 into the ATP-bound state that we have previously demonstrated has high affinity for client proteins.[14]

It should be emphasized that the complex between Hsp90 and p23 is dynamic. The half-time ($t_{1/2}$) for dissociation is approximately 40 s at 37 °C increasing to 4 min at 25 °C. This compares well to $t_{1/2}$ of 2 min at 30 °C for the interaction between human p23 and chicken Hsp90α,[32] and 3 min for the dissociation of Sba1 from yeast Hsp90.AMP-PNP.[33] The dissociation of p23 is an order of magnitude faster than the rate-limiting step of the hydrolysis cycle, which has a $t_{1/2}$ of approximately 7 min.[14] Therefore, if we consider the flux through the pathways that are available to Hsp90, the arrest of the cycle can be overcome by (i) dissociation of p23 and subsequent hydrolysis or (ii) association of additional factors that catalyse the conformational changes that lead to hydrolysis. For example, we have previously observed that, in contrast to the present study, p23 is unable to completely inhibit the ATPase activity of Hsp90 in the presence of a client protein and the immunophilin FKBP52.[13] Instead, p23 represses the client protein-stimulated rate by approximately 90%. Once Hsp90 is in the ADP-bound form it has a lower affinity for both p23 and client protein, so a client may dissociate.

This study adds to the growing evidence that, in comparison to the yeast protein, human Hsp90 is under tighter control. Consequently, the dynamics of the interactions of Hsp90 with client proteins and co-chaperones may differ. Fundamentally, the intrinsic ATPase activity of human Hsp90 is an order of magnitude lower than yeast Hsp90 at the same temperature;[13] and the rate-limiting step does not involve the N-terminal dimerisation for the human protein.[14] There are significant differences between the mechanism of action of human p23 and that of yeast Sba1, which either fails to bind or interacts only weakly with the unbound state of yeast Hsp90. This would lead to an uncompetitive mechanism for inhibition, where Sba1 will enter the yeast Hsp90 cycle at a later stage than human p23 when yeast Hsp90 is in the ATP-bound form. In sharp contrast to human p23, Sba1 inhibits the ATPase activity of yeast Hsp90 only partially.[33,34] The level of sequence identity is 27% in the globular cores of human and yeast p23 compared to 64% identity for the respective Hsp90 homologues. It is possible that sequence variation between the p23 homologues can account for the subtle differences between their interactions leading to a change in the mechanism of inhibition. Similarly, other co-chaperones exhibit different effects on yeast and human Hsp90. The yeast co-chaperone Sti1(HOP) inhibits the basal ATPase activity of yeast Hsp90,[15,52] while the human homologue has no effect on the basal ATPase rate but inhibits the client protein-stimulated rate.[13] The molecular basis of these differences and how p23 and client proteins regulate the Hsp90 ATPase cycle await further analysis.

To summarise, human p23 is monomeric and binds to each subunit of the Hsp90 dimer in both the unbound and nucleotide-bound states, leading to complete inhibition of the ATPase activity following a mixed inhibition model. Association with p23 increases the apparent affinity of Hsp90 for ATP. Thereby, the role of p23 as a Hsp90 co-chaperone is to govern the dynamics of client protein association by preventing the conversion of Hsp90 from the ATP-bound state that has high-affinity for client proteins to the lower affinity ADP-bound form.

Methods

Protein expression and purification

Human Hsp90β and Hsp90ΔC were expressed and purified as described.[13,14] Human p23ΔC was produced by introducing a stop codon at position 623 by site-directed mutagenesis (QuikChange, Stratagene). Human p23 and p23ΔC were expressed as hexahistidine fusions and purified by passage through a nickel-iminodiacetic acid agarose column as described for Hsp90, except the proteins were cleaved *in situ* with bovine thrombin (Sigma). The eluted untagged p23 and p23ΔC were purified by gel-filtration chromatography on a G75 Sepharose HR26/60 column in 50 mM Tris–HCl (pH 7.4), 150 mM NaCl, 10 mM glycerol, 1 mM DTT. The pooled p23 was further purified on a Mono Q HR10/10 column (Pharmacia) equilibrated with 20 mM piperazine (pH 5.2), 10 mM glycerol, 1 mM DTT. Bound protein was eluted with a linear salt gradient over 180 ml from 0–1 M NaCl. The purity of the proteins was determined by SDS-PAGE, mass spectrometry and N-terminal protein sequencing to be greater than 95% (data not shown). Protein concentrations were determined spectrophotometrically and are quoted as monomers.

Surface plasmon resonance

Amine cross-linking was used to attach p23 to the surface of a CM5 sensor chip (Biacore, Uppsala, Sweden) using the protocol supplied by the manufacturer. Measurements were made using chips equilibrated in 40 mM Hepes–KOH (pH 7.5), 20 mM KCl, 6 mM $MgCl_2$, 1 mM DTT, in the presence or in the absence of 2 mM AMP-PNP or 2 mM ADP at 25 °C or 37 °C. For experiments with Hsp90ΔC, glycerol was added to a final concentration of 10% (v/v). The volume of analyte

(Hsp90) injected was 35 µl at a rate of 20 µl/min. The concentration of analyte was varied to test for mass-transport effects. Signal from the p23-coupled cell was compared to that from the blank reference cell. The kinetics of the interactions were analysed using the non-linear regression program Kaleidagraph (version 3.0, Synergy Software, PCS Inc.). The rate constants of dissociation were measured by fitting dissociation data using a single-exponential function. The rate constants of association were obtained by fitting the observed relative change in the resonance signal (R) at time t using the following equation:

$$R = \left(\frac{k_{on}CR_{max}}{k_{on}C + k_{off}}\right)\left[1 - \exp^{-(k_{on}C + k_{off})t}\right] \quad (1)$$

where k_{on} and k_{off} are the association and dissociation rate constants, respectively, C is the analyte concentration and R_{max} is the maximum change in resonance.

Determination of the oligomeric state of p23 and p23ΔC

Analytical size-exclusion chromatography was performed on a Sephadex S75 HR10/30 (Pharmacia) column equilibrated in 50 mM Tris–HCl (pH 8.0), 150 mM NaCl, 1 mM DTT. The relative elution volumes of 100 µl of between 7 µM p23 and p23ΔC were compared with molecular mass standards (Sigma).

The relative elution volume was calculated as:

$$K_{AV} = \frac{V_e - V_o}{V_g - V_o} \quad (2)$$

where V_e is the elution volume, V_o is the void volume determined by elution of blue dextran 2000 (Sigma) and V_g is the geometric column volume. To determine the effect of DTT on the oligomeric status of p23, samples were incubated for 90 min at room temperature in the presence or in the absence of 10 mM DTT before size-exclusion chromatography in the absence of DTT.

Measurement of the free cysteine content of p23 using Ellman's reagent

p23 (400 nM) was incubated in 50 mM Tris–HCl (pH 8.0), 100 µM 5,5′-dithiobis(2-nitrobenzoic acid) in the presence or in the absence of 6 M GdnHCl for 15 min at room temperature. The change in absorbance at 412 nm was used to calculate the concentration of modified cysteine residues using an extinction coefficient of 13, 600 $cm^{-1}\,M^{-1}$.

Analytical ultracentrifugation

Sedimentation equilibrium analysis was performed using a Beckman Optima XL-I analytical ultracentrifuge equipped with absorbance optics, using an An-60Ti rotor at 5 °C. p23 and p23ΔC were dialysed against 50 mM Tris–HCl (pH 7.5), 150 mM NaCl, 10 mM $MgCl_2$, 10 mM KCl, 5 mM Tris (2-carboxyethyl) phosphine(Pierce). Three samples were run simultaneously with initial uniform protein concentrations giving absorbance at 280 nm (A_{280}) values (1 cm path-length) of 0.25, 0.45 and 0.60, respectively. Further concentrations of 130 µM and 150 µM for p23ΔC and p23, respectively, were analysed using data recorded using the Rayleigh interference optics. Dialysis buffer was used as a blank reference. Data were collected at equilibrium for four different angular velocities: 10,000 rpm, 14,000 rpm, 18,000 rpm and 30,000 rpm. The concentration was measured as a function of radial position as A_{280}. Datum points were 0.001 cm apart and the final datum was an average of five measurements. Data analysis was performed using WinNonlin 1.06 (D.A. Yphantis, M.L. Johnson, J.W. Lary, University of Conneticut). Values for the solvent density and protein partial specific volume were calculated using Sednterp (University of New Hampshire) to be 0.7232 g/ml and 1.00175 ml/g, respectively. Concentrations given are based on extinction coefficients of 31,010 $M^{-1}\,cm^{-1}$ for p23 and p23ΔC. Only datum points with an A_{280} value between 0.1 and 1.0 were included in the analysis.

Small-angle X-ray scattering experiments

Small-angle X-ray solution scattering data were collected at station 2.1 of the Daresbury SRS as described.[17]

NanoESI time-of-flight (TOF) MS

Mass spectra were recorded on a tandem mass spectrometer (Q-Tof, Micromass, Manchester, UK) modified for high mass operation.[53] NanoESI-MS capillaries were prepared in-house from borosilicate glass tubes of 1 mm outer diameter and 0.5 mm inner diameter (Harvard Apparatus, Holliston, MA) using a Flaming/Brown P-97 micropipette puller (Sutter Instruments, Hercules, CA) and gold-coated using a sputter coater (Quorum Technologies, Newhaven, UK). The capillary tips were cut under a stereomicroscope to give inner diameters of 1–5 µm, and typically 0.5–2 µl of solution were loaded for sampling. The conditions within the mass spectrometer (specifically pressures and accelerating potentials) were adjusted to preserve non-covalent interactions.[54,55]

External calibration of the spectra was achieved using solutions of cesium iodide. Data were acquired and processed with MassLynx software (Micromass, Manchester, UK). The series of peaks that arise for each species are attributed to different numbers of protons attached to the molecular ion. Their mass-to-charge (m/z) ratios follow the equation:

$$m/z = (M_{protein} + zM_{H+})/z \quad (3)$$

where $M_{protein}$ is the protein mass, M_{H+} is the mass of a proton, and z is the number of protons (charges). Multiple protonation is induced by the electrospray process and occurs up to a maximum corresponding to approximately the number of accessible basic sites in the protein.[56] Transformation of the signal from an m/z to mass scale is performed using MassLynx by multiplication of the m/z value of each peak with the number of charges, z, and subtraction of z times the proton mass. We used tandem MS, where ions are selected by the quadrupole mass analyser of the Q-Tof and subjected to collision-induced dissociation in a gas-filled collision cell to reveal the composition of the non-covalent complexes.[53]

ATPase assay

ATPase activities of purified human Hsp90β and Hsp90ΔC in the absence or in the presence of p23 were measured with a fluorescence-based assay using the Phosphate Binding Protein as described.[13,57] All activities are the averages of three or more separate experiments.

Isothermal titration calorimetry

Isothermal titration calorimetry was performed using a MicroCal VP-ITC instrument (Microcal Inc., Northampton, MA). AMP-PNP (250 μl at 2 mM) in a syringe was injected into a cell containing 50 μM Hsp90 and 125 μM p23 in 50 mM Tris–HCl (pH 7.4), 6 mM $MgCl_2$ 20 mM KCl, 1 mM Tris (2-carboxyethyl) phosphine, at 25 °C. Parallel experiments were carried out by injecting nucleotide into assay buffer without Hsp90 to correct for the heat of dilution in subsequent data analysis using the Origin software package (MicroCal Inc.). Protein and nucleotide concentrations were determined spectrophotometrically.

Acknowledgements

We thank Dr M. Shirouzu (Riken Institute, Japan) for the human Hsp90β plasmid and Dr Martin Webb (NIMR, Mill Hill, UK) for a gift of the PBP expression vector. We acknowledge fruitful discussions with Dr Pam Rowling. We are grateful to Ryan Bentley for technical assistance. This work was funded by a Leverhulme Special Research Fellowship (to S.H.M.), the Newton Trust and the Welton Foundation.

References

1. Mayer, M. P. & Bukau, B. (1999). Molecular chaperones: the busy life of Hsp90. *Curr. Biol.* **9**, R322–R325.
2. Wegele, H., Muller, L. & Buchner, J. (2004). Hsp70 and Hsp90-a relay team for protein folding. *Rev. Physiol. Biochem. Pharmacol.* **151**, 1–44.
3. Pratt, W. B. (1998). The Hsp90-based chaperone system: involvement in signal transduction from a variety of hormone and growth factor receptors. *Proc. Soc. Expt. Biol. Med.* **217**, 420–434.
4. Picard, D. (2002). Heat-shock protein 90, a chaperone for folding and regulation. *Cell Mol. Life Sci.* **59**, 1640–1648.
5. Young, J. C., Moarefi, I. & Hartl, F. U. (2001). Hsp90: a specialized but essential protein-folding tool. *J. Cell Biol.* **154**, 267–273.
6. Zhao, R., Davey, M., Hsu, Y. C., Kaplanek, P., Tong, A., Parsons, A. B. *et al*. (2005). Navigating the chaperone network: an integrative map of physical and genetic interactions mediated by the Hsp90 chaperone. *Cell*, **120**, 715–727.
7. Millson, S. H., Truman, A. W., King, V., Prodromou, C., Pearl, L. H. & Piper, P. W. (2005). A two-hybrid screen of the yeast proteome for Hsp90 interactors uncovers a novel Hsp90 chaperone requirement in the activity of a stress-activated mitogen-activated protein kinase, Slt2p (Mpk1p). *Eukaryot. Cell.* **4**, 849–860.
8. Prodromou, C., Roe, S. M., O'Brien, D. N., Ladbury, J. E., Piper, P. W. & Pearl, L. H. (1997). Identification and structural characterization of the ATP/ADP-binding site in the Hsp90 molecular chaperone. *Cell*, **90**, 65–75.
9. Obermann, W. M. J., Sondermann, H., Russo, A. A., Pavletich, N. P. & Hartl, F. U. (1998). *In vivo* function of Hsp90 is dependent on ATP binding and ATP hydrolysis. *J. Cell Biol.* **143**, 901–910.
10. Prodromou, C., Panaretou, B., Chohan, S., Siligardi, G., O'Brien, R., Ladbury, J. E. *et al*. (2000). The ATPase cycle of Hsp90 drives a molecular 'clamp' *via* transient dimerization of the N-terminal domains. *EMBO J.* **19**, 4383–4392.
11. Sullivan, W., Stensgard, B., Caucutt, G., Bartha, B., McMahon, N., Alnemri, E. S. *et al*. (1997). Nucleotides and two functional states of Hsp90. *J. Biol. Chem.* **272**, 8007–8012.
12. Young, J. C. & Hartl, F. U. (2000). Polypeptide release by Hsp90 involves ATP hydrolysis and is enhanced by the co-chaperone p23. *EMBO J.* **19**, 5930–5940.
13. McLaughlin, S. H., Smith, H. W. & Jackson, S. E. (2002). Stimulation of the weak ATPase activity of human Hsp90 by a client protein. *J. Mol. Biol.* **315**, 787–798.
14. McLaughlin, S. H., Ventouras, L.-A., Lobbezoo, B. & Jackson, S. E. (2004). Independent ATPase activity of Hsp90 subunits creates a flexible assembly platform. *J. Mol. Biol.* **344**, 813–826.
15. Richter, K., Muschler, P., Hainzl, O., Reinstein, J. & Buchner, J. (2003). Sti1 is a non-competitive inhibitor of the Hsp90 ATPase. Binding prevents the N-terminal dimerization reaction during the ATPase cycle. *J. Biol. Chem.* **278**, 10328–10333.
16. Siligardi, G., Panaretou, B., Meyer, P., Singh, S., Woolfson, D. N., Piper, P. W. *et al*. (2002). Regulation of Hsp90 ATPase activity by the co-chaperone Cdc37p/p50cdc37. *J. Biol. Chem.* **277**, 20151–20159.
17. Zhang, W., Hirshberg, M., McLaughlin, S. H., Lazar, G. A., Grossmann, J. G., Nielsen, P. R. *et al*. (2004). Biochemical and structural studies of the interaction of Cdc37 with Hsp90. *J. Mol. Biol.* **340**, 891–907.
18. Johnson, J. L., Beito, T. G., Krco, C. J. & Toft, D. O. (1994). Characterization of a novel 23-kilodalton protein of unactive progesterone receptor complexes. *Mol. Cell. Biol.* **14**, 1956–1963.
19. Johnson, J. L. & Toft, D. O. (1994). A novel chaperone complex for steroid receptors involving heat shock proteins, immunophilins, and p23. *J. Biol. Chem.* **269**, 24989–24993.
20. Hutchison, K. A., Stancato, L. F., Owens-Grillo, J. K., Johnson, J. L., Krishna, P., Toft, D. O. & Pratt, W. B. (1995). The 23-kDa acidic protein in reticulocyte lysate is the weakly bound component of the hsp foldosome that is required for assembly of the glucocorticoid receptor into a functional heterocomplex with Hsp90. *J. Biol. Chem.* **270**, 18841–18847.
21. Toft, D. O. (1998). Recent advances in the study of Hsp90 structure and mechanism of action. *Trends Endocrinol. Metab.* **9**, 238–243.
22. Smith, D. F. (2000). Chaperones in progesterone receptor complexes. *Semin. Cell Dev. Biol.* **11**, 45–52.
23. Dittmar, K. D., Demady, D. R., Stancato, L. F., Krishna, P. & Pratt, W. B. (1997). Folding of the glucocorticoid receptor by the heat shock protein (hsp) 90-based chaperone machinery. The role of p23 is to stabilize receptor.hsp90 heterocomplexes formed by hsp90.p60.hsp70. *J. Biol. Chem.* **272**, 21213–21220.
24. Kosano, H., Stensgard, B., Charlesworth, M. C., McMahon, N. & Toft, D. (1998). The assembly of progesterone receptor-Hsp90 complexes using purified proteins. *J. Biol. Chem.* **273**, 32973–32979.
25. Knoblauch, R. & Garabedian, M. J. (1999). Role for Hsp90-associated cochaperone p23 in estrogen receptor signal transduction. *Mol. Cell. Biol.* **19**, 3748–3759.
26. Bose, S., Weikl, T., Bugl, H. & Buchner, J. (1996). Chaperone function of Hsp90-associated proteins. *Science*, **274**, 1715–1717.
27. Freeman, B. C., Toft, D. O. & Morimoto, R. I. (1996). Molecular chaperone machines: chaperone activities

of the cyclophilin Cyp-40 and the steroid aporeceptor-associated protein p23. *Science*, **274**, 1718–1720.
28. Freeman, B. C., Felts, S. J., Toft, D. O. & Yamamoto, K. R. (2000). The p23 molecular chaperones act at a late step in intracellular receptor action to differentially affect ligand efficacies. *Genes Dev.* **14**, 422–434.
29. Bohen, S. P. (1998). Genetic and biochemical analysis of p23 and ansamycin antibiotics in the function of Hsp90-dependent signaling proteins. *Mol. Cell. Biol.* **18**, 3330–3339.
30. Fang, Y., Fliss, A. E., Rao, J. & Caplan, A. J. (1998). SBA1 encodes a yeast hsp90 cochaperone that is homologous to vertebrate p23 proteins. *Mol. Cell. Biol.* **18**, 3727–3734.
31. Johnson, J. L. & Toft, D. O. (1995). Binding of p23 and Hsp90 during assembly with the progesterone receptor. *Mol. Endocrinol.* **9**, 670–678.
32. Sullivan, W. P., Owen, B. A. & Toft, D. O. (2002). The influence of ATP and p23 on the conformation of Hsp90. *J. Biol. Chem.* **277**, 45942–45948.
33. Richter, K., Walter, S. & Buchner, J. (2004). The co-chaperone Sba1 connects the ATPase reaction of Hsp90 to the progression of the chaperone cycle. *J. Mol. Biol.* **342**, 1403–1413.
34. Siligardi, G., Hu, B., Panaretou, B., Piper, P. W., Pearl, L. H. & Prodromou, C. (2004). Co-chaperone regulation of conformational switching in the Hsp90 ATPase cycle. *J. Biol. Chem.* **279**, 51989–51998.
35. Zhu, S. & Tytgat, J. (2004). Evolutionary epitopes of Hsp90 and p23: implications for their interaction. *FASEB J.* **18**, 940–947.
36. Oxelmark, E., Knoblauch, R., Arnal, S., Su, L. F., Schapira, M. & Garabedian, M. J. (2003). Genetic dissection of p23, an Hsp90 cochaperone, reveals a distinct surface involved in estrogen receptor signaling. *J. Biol. Chem.* **278**, 36547–36555.
37. Wochnik, G. M., Young, J. C., Schmidt, U., Holsboer, F., Hartl, F. U. & Rein, T. (2004). Inhibition of GR-mediated transcription by p23 requires interaction with Hsp90. *FEBS Letters*, **560**, 35–38.
38. Chadli, A., Bouhouche, I., Sullivan, W., Stensgard, B., McMahon, N., Catelli, M. G. & Toft, D. O. (2000). Dimerization and N-terminal domain proximity underlie the function of the molecular chaperone heat shock protein 90. *Proc. Natl Acad. Sci. USA*, **97**, 12524–12529.
39. Harris, S. F., Shiau, A. K. & Agard, D. A. (2004). The crystal structure of the carboxy-terminal dimerization domain of hptG, the *Escherichia coli* Hsp90, reveals apotential substrate binding site. *Structure*, **12**, 1087–1097.
40. Weaver, A. J., Sullivan, W. P., Felts, S. J., Owen, B. A. & Toft, D. O. (2000). Crystal structure and activity of human p23, a heat shock protein 90 co-chaperone. *J. Biol. Chem.* **275**, 23045–23052.
41. Weikl, T., Abelmann, K. & Buchner, J. (1999). An unstructured C-terminal region of the Hsp90 co-chaperone p23 is important for its chaperone function. *J. Mol. Biol.* **293**, 685–691.
42. Grenert, J. P., Johnson, B. D. & Toft, D. O. (1999). The importance of ATP binding and hydrolysis by Hsp90 in formation and function of protein heterocomplexes. *J. Biol. Chem.* **274**, 17525–17533.
43. Wigley, D. B., Davies, G. J., Dodson, E. J., Maxwell, A. & Dodson, G. (1991). Crystal structure of an N-terminal fragment of the DNA gyrase B protein. *Nature*, **351**, 624–629.
44. Richter, K., Muschler, P., Hainzl, O. & Buchner, J. (2001). Coordinated ATP hydrolysis by the Hsp90 dimer. *J. Biol. Chem.* **276**, 33689–33696.
45. Meyer, P., Prodromou, C., Hu, B., Vaughan, C., Roe, S. M., Panaretou, B. *et al*. (2003). Structural and functional analysis of the middle segment of Hsp90. Implications for ATP hydrolysis and client protein and cochaperone interactions. *Mol. Cell.* **11**, 647–658.
46. Huai, Q., Wang, H., Liu, Y., Kim, H. Y., Toft, D. & Ke, H. (2005). Structures of the N-terminal and middle domains of *E. coli* Hsp90 and conformation changes upon ADP binding. *Structure*, **13**, 579–590.
47. Roe, S. M., Ali, M. M., Meyer, P., Vaughan, C. K., Panaretou, B., Piper, P. W. *et al*. (2004). The mechanism of Hsp90 regulation by the protein kinase-specific cochaperone p50(Cdc37). *Cell*, **116**, 87–98.
48. Harst, A., Lin, H. & Obermann, W. M. (2005). Aha1 competes with Hop, p50 and p23 for binding to the molecular chaperone Hsp90 and contributes to kinase and hormone receptor activation. *Biochem. J.* **387**, 789–796.
49. Hartson, S. D., Irwin, A. D., Shao, J., Scroggins, B. T., Volk, L., Huang, W. & Matts, R. L. (2000). $p50^{cdc37}$ is a nonexclusive Hsp90 cohort which participates intimately in Hsp90-mediated folding of immature kinase molecules. *Biochemistry*, **39**, 7631–7644.
50. Meyer, P., Prodromou, C., Liao, C., Hu, B., Mark Roe, S., Vaughan, C. K. *et al*. (2004). Structural basis for recruitment of the ATPase activator Aha1 to the Hsp90 chaperone machinery. *EMBO J.* **23**, 1402–1410.
51. Abbas-Terki, T., Briand, P. A., Donze, O. & Picard, D. (2002). The Hsp90 co-chaperones Cdc37 and Sti1 interact physically and genetically. *Biol. Chem.* **383**, 1335–1342.
52. Prodromou, C., Siligardi, G., O'Brien, R., Woolfson, D. N., Regan, L., Panaretou, B. *et al*. (1999). Regulation of Hsp90 ATPase activity by tetratricopeptide repeat (TPR)-domain co-chaperones. *EMBO J.* **18**, 754–762.
53. Sobott, F., Hernandez, H., McCammon, M. G., Tito, M. A. & Robinson, C. V. (2002). A tandem mass spectrometer for improved transmission and analysis of large macromolecular assemblies. *Anal. Chem.* **74**, 1402–1407.
54. Sobott, F. & Robinson, C. V. (2002). Protein complexes gain momentum. *Curr. Opin. Struct. Biol.* **12**, 729–734.
55. Heck, A. J. & Van Den Heuvel, R. H. (2004). Investigation of intact protein complexes by mass spectrometry. *Mass Spectrom. Rev.* **23**, 368–389.
56. Kebarle, P. (2000). A brief overview of the present status of the mechanisms involved in electrospray mass spectrometry. *J. Mass Spectrom.* **35**, 804–817.
57. Brune, M., Hunter, J. L., Howell, S. A., Martin, S. R., Hazlett, T. L., Corrie, J. E. T. & Webb, M. R. (1998). Mechanism of inorganic phosphate interaction with phosphate binding protein from *Escherichia coli*. *Biochemistry*, **37**, 10370–10380.

Edited by M. Gottesman

(Received 9 September 2005; received in revised form 25 November 2005; accepted 28 November 2005)
Available online 15 December 2005